Nucl. Fusion **47** (2007) S1–S17 doi:10.1088/0029-5515/47/6/S01

Chapter 1: Overview and summary

Editors of 'Progress in the ITER Physics Basis':
M. Shimada[1,a], D.J. Campbell[1,2], V. Mukhovatov[1], M. Fujiwara[3], N. Kirneva[4], K. Lackner[5], M. Nagami[6], V.D. Pustovitov[4], N. Uckan[7] and J. Wesley[8]
International Tokamak Physics Activity Topical Group Chairs, Cochairs and Chapter Coordinators:
N. Asakura[6], A.E. Costley[1], A.J.H. Donné[9], E.J. Doyle[10], A. Fasoli[11], C. Gormezano[12,13], Y. Gribov[1], O. Gruber[5], T.C. Hender[14], W. Houlberg[7], S. Ide[6], Y. Kamada[6], A. Leonard[8], B. Lipschultz[15], A. Loarte[2], K. Miyamoto[13,16], V. Mukhovatov[1], T.H. Osborne[8], A. Polevoi[1] and A.C.C. Sips[5]

[1] ITER Organization
[2] European Fusion Development Agreement Close Support Unit-Garching
[3] National Institute for Fusion Studies, Japan
[4] Kurchatov Institute, Russia
[5] Institut für Plasmaphysik, Garching, Germany
[6] Japan Atomic Energy Agency, Naka, Japan
[7] Oak Ridge National Laboratories, USA
[8] General Atomics, USA
[9] FOM-Institute for Plasma Physics Rijnhuizen, Netherlands
[10] University of California, Los Angeles, USA
[11] Centre de Recherches en Physique des Plasmas, Ecole Polytechnique Fédérale, Switzerland
[12] Ente per le Nuove tecnologie, l'Energia e l'Ambiente, Italy
[13] Retired
[14] United Kingdom Atomic Energy Authority, Abingdon, UK
[15] Plasma Science and Fusion Center, Massachusetts Institute of Technology, USA
[16] University of Tokyo, Japan

E-mail: michiya.shimada@iter.org

Received 6 November 2006, accepted for publication 30 April 2007
Published 1 June 2007
Online at stacks.iop.org/NF/47/S1

Abstract
The 'Progress in the ITER Physics Basis' (PIPB) document is an update of the 'ITER Physics Basis' (IPB), which was published in 1999 [1]. The IPB provided methodologies for projecting the performance of burning plasmas, developed largely through coordinated experimental, modelling and theoretical activities carried out on today's large tokamaks (ITER Physics R&D). In the IPB, projections for ITER (1998 Design) were also presented. The IPB also pointed out some outstanding issues. These issues have been addressed by the Participant Teams of ITER (the European Union, Japan, Russia and the USA), for which International Tokamak Physics Activities (ITPA) provided a forum of scientists, focusing on open issues pointed out in the IPB. The new methodologies of projection and control are applied to ITER, which was redesigned under revised technical objectives. These analyses suggest that the achievement of $Q > 10$ in the inductive operation is feasible. Further, improved confinement and beta observed with low shear (= high β_p = 'hybrid') operation scenarios, if achieved in ITER, could provide attractive scenarios with high $Q(> 10)$, long pulse (>1000 s) operation with beta <no-wall limit and benign ELMs.

PACS numbers: 28.52.−s, 52.55.Fa, 52.55.−s, 52.40.Hf

(Some figures in this article are in colour only in the electronic version)

[a] Author to whom any correspondence should be addressed.

Contents

1. Introduction

The objective of ITER is to demonstrate the scientific and technological feasibility of fusion energy for peaceful purposes. Its inductive operation is expected to produce significant fusion power (~500 MW) through the D–T reaction with high fusion gain $Q \sim 10$ (the ratio of fusion power to the external heating power) for 300–500 s. In other words, the majority of the heating power will be provided by alpha particle heating and the plasma largely determines its own profiles. ITER will be the first device in which this autonomous plasma state is achieved. ITER will also aim at steady-state, high gain operation lasting for ~3000 s. In steady-state plasmas, a large fraction (>50%) of the plasma current will be driven by spontaneous bootstrap current originating from the pressure gradient, which enhances the degree of plasma autonomy. Impurity levels are also determined self-consistently by plasma processes, such as sputtering, screening, transport and radiative cooling: for example, excessive impurity levels would limit the fusion reaction through dilution and radiative cooling, which would then reduce the impurity concentration to an equilibrium level. Since helium particles (alpha particles) are created by the fusion reactions, the determination of impurity levels will be more complex in fusion plasmas. Engineering tests of reactor-relevant components, such as breeding blankets, are also an important mission of ITER, and require a reliable operation scheme with significant fusion power and long pulses (>1000 s). Projection studies show that such scenarios are possible with a modest requirement on confinement and beta (hybrid scenarios, which combine inductive and non-inductive current drive at a plasma current lower than the inductive scenarios). While the physics basis for ITER's nominal inductive operation is relatively well established, the projection of plasma performance is associated with some uncertainty, due to extrapolation of parameters to regimes unattainable in present machines, and experiments in ITER are needed to lay the foundation for the operation of demonstration power reactors (Demo) that will follow ITER.

The present ITER design stems from more than 15 years of joint magnetic fusion reactor design activities and supporting physics and technology research by the four original ITER parties—the European Union (EU), Japan (JA), the Russian Federation (RF) and the United States of America (US)—who are now joined by China, India and Korea in the collaborative international effort to construct the ITER tokamak device. For 3 years Canada was also a partner. Present plans call for first operation of ITER to commence 8.5 years after the start of construction.

Physics understanding and methodologies of projection and control of such burning plasmas must be based on experimental, modelling and theoretical research. The Progress in the ITER Physics Basis (PIPB) that follows in chapter 2-9 of this issue consists of updates to the physics basis for a burning plasma tokamak that was presented in the ITER Physics Basis (IPB) [1]. As the title of that document implies, the content of the IPB comprises an extensive compilation of the physics basis for the design and operation of a burning-plasma-capable tokamak, specifically the 1998 embodiment [2,3] of the International Thermonuclear Experimental Reactor (ITER). Physics research after the IPB has been carried out by four participating parties (EU, JA, RF and US). The International Tokamak Physics Activity (ITPA) provided an excellent forum focusing on open issues pointed out in the IPB, which has made significant progress. The PIPB provides an update—focusing on progress obtained since 1998—to the physics basis considerations identified in the IPB and presents application of those considerations to the current embodiment of the ITER design [4]. It also discusses the role of ITER in the strategy of fusion reactor development (chapter 9 of this issue [5]).

This chapter will provide an introduction and outline of the complete PIPB document. The mission, objectives and technical attributes of the design are described in detail in [4] and will be shown briefly in section 2 and described in greater detail in appendix A. In section 3, the progress in the understanding of physical processes and methodologies

for projection and control since the IPB are summarized. In section 4, conclusions are presented.

2. ITER objectives and capabilities

The objective for ITER is to demonstrate the scientific and technological feasibility of applying fusion energy for peaceful purposes. In more direct terms, ITER will, for the first time, be able to produce a 'burning' deuterium–tritium plasma—that is one where the majority of the heating needed to sustain the fusion reaction is self-produced from fusion-generated alpha particles. The production and control of such a self-heated plasma has been the long-standing goal for more than 50 years of magnetic fusion research.

In 1998, six years of joint work originally foreseen under the ITER engineering design activities (EDA) agreement culminated in a design [2] fulfilling all objectives and the cost target adopted by the ITER parties (the European Union, Japan, Russia and the US) in 1992 at the start of the EDA. However, for financial reasons, the ITER parties recognized the need of a new design to meet revised technical objectives and a cost reduction target of about 50% of the previously accepted cost estimate. The joint central team and home teams elaborated revised technical objectives. The revised performance specifications adopted by the ITER Council in June 1998 [6] are set out in full in table 1; in summary they require ITER:

- to achieve extended burn in inductively driven deuterium–tritium (DT) plasma operation with $Q \geqslant 10$, not precluding ignition (i.e. the plasma is sustained by fusion reactions only and without auxiliary power injected), with a burn duration of between 300 and 500 s;
- to aim at demonstrating steady-state operation using non-inductive current drive with $Q \geqslant 5$.

In terms of engineering performance and testing, the design should:

- demonstrate availability and integration of essential fusion technologies,
- test components for a future reactor and
- test tritium breeding module concepts; with a 14 MeV neutron power load on the first wall $\geqslant 0.5\,\mathrm{MW\,m^{-2}}$ and fluence $\geqslant 0.3\,\mathrm{MWa\,m^{-2}}$.

In addition, the device should:

- use as far as possible technical solutions and concepts developed and qualified during the previous period of the EDA and
- cost about 50% of the direct capital cost of the 1998 ITER design.

The new ITER design, whilst having reduced technical objectives from its predecessor, will nonetheless meet the programmatic objective of providing an integrated demonstration of the scientific and technological feasibility of fusion energy. Further, the standard operation regime of ITER of the 1998 design assumed electron densities higher than the Greenwald density. This raised a concern, since many tokamaks exhibited deterioration of energy confinement as the density approached the Greenwald density. The standard operation regime of the new ITER is at or below the Greenwald density, which improved the feasibility of achieving ITER's goals. But since ITER will operate at $Q \sim 10$ and fusion power of ~500 MW, there will still be an extrapolation to power reactors ($Q \sim 50$ and fusion power of ~3 GW).

ITER is based on the tokamak concept [7]. A combination of an externally-generated toroidal magnetic field and the poloidal magnetic field, generated by toroidal current flowing in the plasma and coils wound toroidally around the torus, forms a configuration of nested magnetic flux surfaces that is capable of stably supporting the 0.7 MPa (= 7 atm) thermal pressure required for a self-heated 500 MW DT plasma. The ITER design incorporates superconducting magnet systems, water-cooled divertor and plasma-facing first wall and nuclear shield systems that are magnetically and thermally capable of supporting long pulse burning plasma operation (burn pulse durations of 7 min or more). Figure 1 shows a cut-away depiction of the ITER device. Table 2 summarizes the main design features and operational capabilities.

The ITER facility will provide the capabilities for achieving sustained fusion burn in DT plasma with fusion energy gain Q in the range $Q \sim 5$–20. This range of Q, which corresponds to an alpha-heating fraction $f_\alpha = Q/(Q+5)$ of 50–80%, spans the range of f_α needed for physics studies of self-heated plasmas to the higher f_α projected to be needed for a future power-producing tokamak fusion reactor.

With ITER, it will be possible to investigate a wide spectrum of new phenomena arising from the full nonlinear interplay between α-particle heating, transport, stability, pressure and current profile control, and their compatibility with a divertor and plasma-facing materials in steady-state conditions. These new phenomena could become more complex due to plasma autonomy in plasma profiles, current density and impurity levels as discussed earlier. These new phenomena will excite high academic interest and could pose challenges. However, through investigation of new phenomena, physics understanding will progress and operational regimes attractive for a reactor could be developed.

The operational capabilities of ITER will ultimately depend on the plasma performance that can be obtained and on the degree that the plasma current can be sustained by non-inductive means, i.e. other than continuing to increase the magnetic flux supplied by the central solenoid (CS). Present plans envision that ITER will be capable of operating with three possible modes of plasma operation (commonly described as operation 'scenarios') that will encompass an increasing degree of non-inductive current drive capability and hence achievable burn pulse duration. Table 3 details some of the physics and operational attributes of these three types of operation scenario.

The physics considerations that underlie the design of these three categories of scenarios are fully explained in various ITER design documents and publications and are further addressed in chapters 2–8 of this issue. But briefly put, as table 3 demonstrates, the progress from limited-duration inductively driven burn in the 15 MA 'ELMy H-mode' scenario to the indefinitely sustainable burn possible in the steady-state scenario is marked by a progressive decrease in total plasma current, a corresponding progression in non-inductive current drive fraction, increasing normalized confinement

Table 1. ITER detailed technical objectives and performance specifications (from the ITER Special Working Group Report to the ITER Council on Task #1 results [6]).

Plasma performance
The device should:

- achieve extended burn in inductively driven plasmas with the ratio of fusion power to auxiliary heating power of at least 10 for a range of operating scenarios and with a duration sufficient to achieve stationary conditions on the timescales characteristic of plasma processes;
- aim at demonstrating steady-state operation using non-inductive current drive with the ratio of fusion power to input power for current drive of at least 5.

In addition, the possibility of controlled ignition should not be precluded.

Engineering performance and testing
The device should:

- demonstrate the availability and integration of technologies essential for a fusion reactor (such as superconducting magnets and remote maintenance);
- test components for a future reactor (such as systems to exhaust power and particles from the plasma);
- test tritium breeding module concepts that would lead in a future reactor to tritium self-sufficiency, the extraction of high grade heat and electricity production.

Design requirements

- Engineering choices and design solutions should be adopted which implement the above performance requirements and make maximum appropriate use of existing R&D database (technology and physics) developed for ITER;
- The choice of machine parameters should be consistent with margins that give confidence in achieving the required plasma and engineering performance in accordance with physics design rules documented and agreed upon by the ITER physics expert groups (predecessor of ITPA Topical Groups);
- The design should be capable of supporting advanced modes of plasma operation under investigation in existing experiments, and should permit a wide operating parameter space to allow for optimizing plasma performance;
- The design should be confirmed by the scientific and technological database available at the end of the EDA;
- In order to satisfy the above plasma performance requirements an inductive flat-top capability during burn of 300–500 s, under nominal operating conditions, should be provided;
- In order to limit the fatigue of components, operation should be limited to a few tens of thousands of pulses;
- In view of the goal of demonstrating steady-state operation using non-inductive current drive in reactor-relevant regimes, the machine design should be able to support equilibria with high bootstrap current fraction and plasma heating dominated by α-particles;
- To carry out nuclear and high heat flux component testing relevant to a future fusion reactor, the engineering requirements are

$$\text{average neutron flux} \geqslant 0.5\,\text{MW m}^{-2}$$
$$\text{average fluence} \geqslant 0.3\text{MWam}^{-2};$$

- The option for later installation of a tritium breeding blanket on the outboard of the device should not be precluded;
- The engineering design choices should be made with the objective of achieving the minimum cost device that meets all the stated requirements.

Operation requirements
The operation should address the issues of burning plasma, steady-state operation and improved modes of confinement and testing of blanket modules.

- Burning plasma experiments will address confinement, stability, exhaust of helium ash and impurity control in plasmas dominated by α-particle heating;
- Steady-state experiments will address issues of non-inductive current drive and other means for profile and burn control and for achieving improved modes of confinement and stability;
- Operating modes should be determined having sufficient reliability for nuclear testing. Provision should be made for low-fluence functional tests of blanket modules to be conducted early in the experimental programme. Higher fluence nuclear tests will be mainly dedicated to DEMO-relevant blanket modules in the above flux and fluence conditions;
- In order to execute this programme, the device is anticipated to operate over an approximately 20-year period. Planning for operation must provide for an adequate tritium supply. It is assumed that there will be an adequate supply from external sources throughout the operational life.

(H98(y,2) factor, the energy confinement time normalized by the H98(y,2) scaling), increasing normalized plasma beta (β_N) and burn time. Here, β is the plasma pressure normalized by magnetic pressure. The normalized plasma beta β_N is the beta normalized by the Troyon scaling ($I_p/(aB)$ in %, I_p (plasma current) in MA, a (plasma horizontal minor radius) in m and B (toroidal magnetic field) in T). The ITER steady-state scenario can be represented as being prototypical of the steady-state scenarios being advocated for future fusion power reactor designs. 'ELMy H-mode' is a discharge mode with improved confinement of energy and particles. It is characterized by a steep gradient in plasma pressure at a radial zone (called edge pedestal), typically several cm wide inside the separatrix surface. Its reduced transport is explained by $E \times B$ shear. It is often associated with periodical bursts of energy and particle due to instability (edge localized mode, ELM), localized around the edge pedestal. The density and temperature at the pedestal top provide boundary conditions of the core plasma, characterizing the plasma performance in the case the profile is stiff.

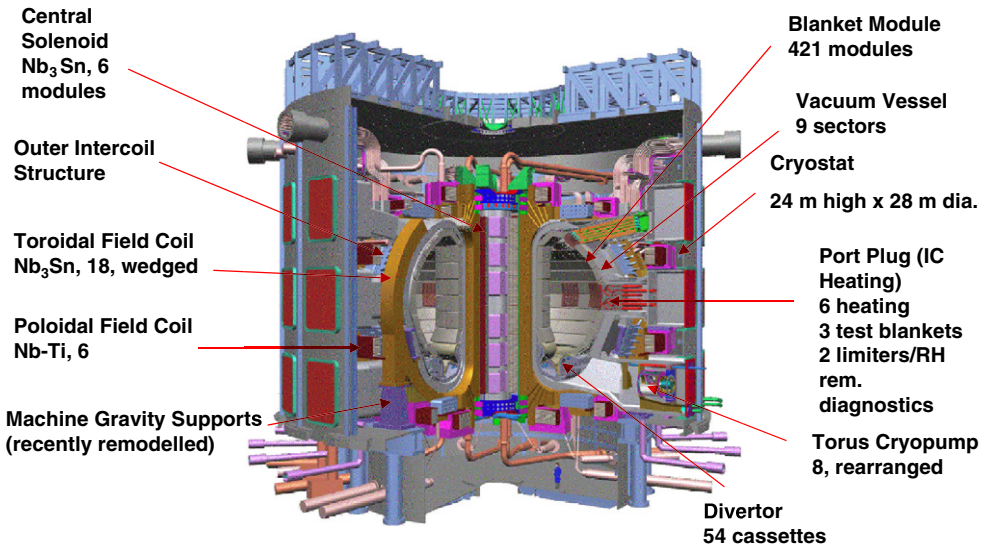

Figure 1. ITER tokamak and major components.

Table 2. ITER parameters and operational capabilities.

Parameter	Attributes
Fusion power	500 MW (700 MW)[a]
Fusion power gain (Q)	$\geqslant$10 (for 400 s inductively driven burn); $\geqslant$5 (steady-state objective)
Plasma major radius (R)	6.2 m
Plasma minor radius (a)	2.0 m
Plasma vertical elongation (95% flux surface/separatrix)	1.70/1.85
Plasma triangularity (95% flux surface/separatrix)	0.33/0.48
Plasma current (I_p)	15 MA (17 MA)[a]
Safety factor at 95% flux surface	3 (at I_p of 15 MA)
Toroidal field at 6.2 m radius	5.3 T
Installed auxiliary heating/ current-drive power	73 MW (110 MW)[b]
Plasma volume	830 m^3
Plasma surface area	680 m^2
Plasma cross section area	22 m^2

[a] Increase possible with limitation on burn duration.
[b] A total plasma heating power of 110 MW may be installed in subsequent operation phases.

Plasma current profiles allow us to classify scenarios for ITER, since the safety factor q profile seems to be the dominant parameter, although several physics phenomena are involved, often interlinked, and have to be taken into account. The safety factor is defined by $q = \mathrm{d}\Psi/\mathrm{d}\Phi$, where Ψ is the toroidal flux and Φ is the poloidal flux enclosed by the magnetic surface. In simpler terms, at a rational q surface, q is the ratio of the number of toroidal turns to the number of poloidal turns of a field line. In other words, q is inversely proportional to the rotational transform, i.e. the pitch or twist of the field line; q is inversely proportional to the average current density inside the volume enclosed in a flux surface. Figure 2 illustrates the variation of safety factor profiles observed in tokamak experiments. In the reference H-mode scenario for ITER, the plasma current is fully diffused and the q profile is monotonic with a large positive magnetic shear.

Here the magnetic shear s is defined as $s = (r/q)\mathrm{d}q/\mathrm{d}r$. In a discharge with a positive magnetic shear, the current density peaks on the centre (magnetic axis), monotonously decreasing with radius. In a discharge with a reverse magnetic shear, the current density has a maximum at an off-axis position. In a discharge with a weak magnetic shear, the current density is almost constant from the centre up to typically about the half minor radius.

Configurations with moderate or weak reversed shear have permitted the development of plasmas whose characteristics are close to the one required for steady-state scenarios: full non-inductive current, high confinement and high bootstrap fraction (section 3.7, chapter 2 [8], chapter 6 [9]). They are also characterized by the development of internal transport barriers when proper conditions are met. Internal transport barrier is a zone in the plasma core with a steep gradient in plasma pressure. More recently, the development of magnetic configurations with a wide volume of low magnetic shear and a central value of q close to 1 has resulted in quasi-stationary discharges with improved confinement and high values of normalized beta. They are also characterized by a low level of MHD activity. These discharges extrapolate to the performance needed for the 'hybrid' scenarios foreseen for ITER.

As was described in the IPB, there are a number of physics basis considerations that are applicable to all three of the proposed ITER scenarios, and there are also other physics basis considerations that are directly relevant to only one or two of the scenarios. These scenario relevancy aspects enter in the presentation of key issues and progress that follows below and into the detailed discussion of PIPB that appears in chapters 2–8 of this issue.

3. Progress in key physics issues and its impact on the choice of the main design parameters of ITER

What follows below are brief narrative accounts of the status and progress in key elements that collectively comprise the body of the physics basis for a burning plasma tokamak and

Table 3. ITER operation scenarios.

Scenario	Plasma current (MA)	Non-inductive fraction	H98(y,2)	li	β_N	Burn duration (s)
Inductive (Scenario 2)	15	0.15	1.0	0.8	1.8	~400
Hybrid (Scenario 3)	~12	~0.50	1–1.2	0.9	2–2.5	⩾1000
Steady-state (Scenario 4)	~ 9	1.00	⩾1.3	0.6	⩾2.6	3000[a]

[a] 3000 s limit is imposed by the cooling system.

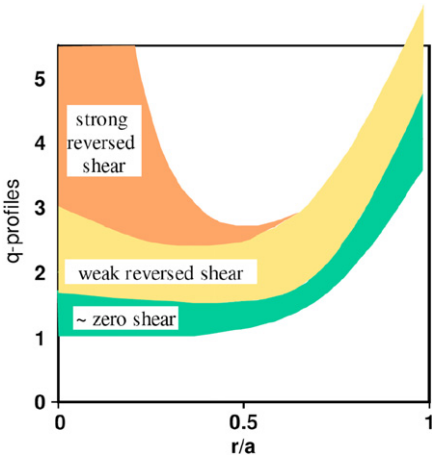

Figure 2. q profiles.

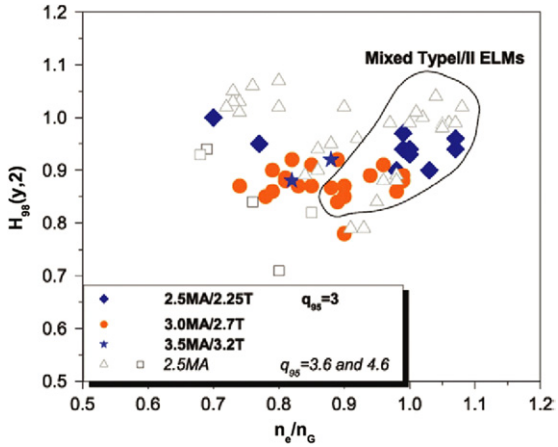

Figure 3. H-factor versus normalized density for the I_P scan and q_{95} scan in JET [11] (chapter 2, section 4.1.3 [8]). Diamonds are discharges with $I_p = 2.5$ MA and $B_t = 2.25$ T ($q_{95} = 3$). Solid circles are discharges with $I_p = 3.0$ MA and $B_t = 2.7$ T. Stars are discharges with $I_p = 3.5$ MA and $B_t = 3.2$ T. Open triangles are discharges with $I_p = 2.5$ MA and $q_{95} = 3.6$. Open squares are discharges with $I_p = 2.5$ MA and $q_{95} = 4.6$.

ITER. The projection to ITER is discussed where possible. The summary accounts given here are necessarily brief. Full scientific details and consideration of many additional aspects of physics basis progress will be found in chapters 2–9 and references therein of this issue.

3.1. Core confinement and transport

At the time of IPB, the main approach used in predicting the performance of ITER in its main regime of operation, the steady H-mode, was the global energy confinement time scaling approach. Here, global energy confinement time is defined as $W/(P - \mathrm{d}W/\mathrm{d}t)$, where W is thermal energy stored in the plasma and P is the total heating power (i.e. the sum of alpha-heating power and auxiliary heating power). Five empirical log-linear (power law) scaling expressions for the energy confinement time were presented in the IPB [10]. The Confinement Database and Modelling Expert Group recommended the IPB98(y,2) scaling as reference scaling for ITER design. Thermal energy confinement time is described by the IPB98(y,2) scaling as

$$\tau_{\mathrm{E,th}}^{\mathrm{IPB\,98}(y,2)} = 0.05621 I_{\mathrm{p}}^{0.93} B_{\mathrm{T}}^{0.15} P^{-0.69} n_{\mathrm{e}}^{0.41} M^{0.19} R^{1.97} \varepsilon^{0.58} \kappa_x^{0.78}, \quad (3.1\text{-}1)$$

where I_p is the plasma current, B_T is the toroidal field (TF), n_e is the volume-averaged density, M is the averaged mass number, R is the major radius and ε is the aspect ratio (a/R, a is the horizontal minor radius). The units are (s, MA, T, MW, $10^{19}\,\mathrm{m}^{-3}$, AMU, m) and the elongation κ_x is defined as $\kappa_x = S_o/(\pi a^2)$ with S_o the plasma cross-sectional area (chapter 2, section 5.3 [8]). The energy confinement time predicted for ITER is 3.7 s. The standard deviation of the residuals for the standard data set with respect to IPB98(y,2) is +14%/ − 13%.

Confinement degradation relative to scaling prediction was observed at densities close to the Greenwald density $n_G = I/\pi a^2$ (where the units are $10^{20}\,\mathrm{m}^{-3}$, MA, m), which was a concern pointed out in IPB (chapter 2, section 5.3.2 [8]). However, recent experiments on many tokamaks demonstrate that a good H-mode confinement can be obtained at densities close to or exceeding the Greenwald density by increasing the triangularity of the plasma cross section and by using pellet injection or impurity gas puffing (figure 3) [11] (chapter 2, section 4.1.3 [8]).

The improved confinement mode, H-mode, is characterized by an abrupt reduction in heat and particle transport originating at the plasma edge (pedestal) and propagating into the core. Experiments show that this transition requires some level of heating power (threshold power). The main approach to the projection of the H-mode threshold power P_{thr} in future large devices is at present a derivation of empirical scalings for P_{thr} expressed in global plasma and device parameters, since a tested quantitative theory is not yet available (chapter 2, section 4.3 [8]). Using an improved and expanded database, the latest projection for ITER is a threshold power in the range of ~50 MW, within the capability of the ITER heating system (73 MW). However, there is uncertainty in the projection and experiments suggest that heating powers ~50% above the threshold power appear to be required to reach good H-mode confinement. This indicates the need of further investigation in this area.

The transport of plasma heat, momentum and particles is enhanced over the prediction from collisional transport theory

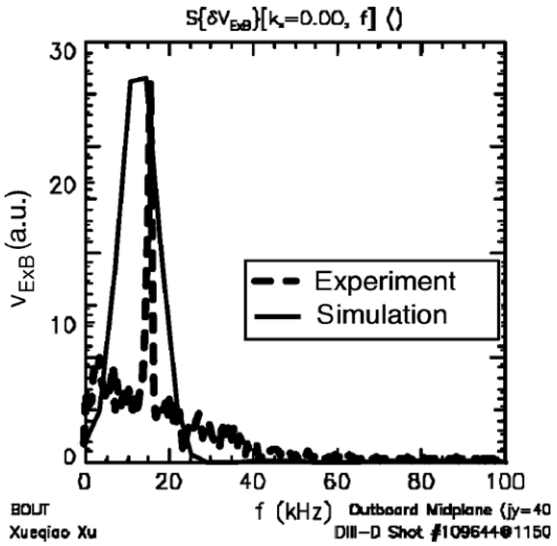

Figure 4. A comparison of a GAM $E \times B$ oscillation observed in a turbulence simulation of experimental discharge using the BOUT code and a comparison with measured turbulence poloidal velocity spectrum [12].

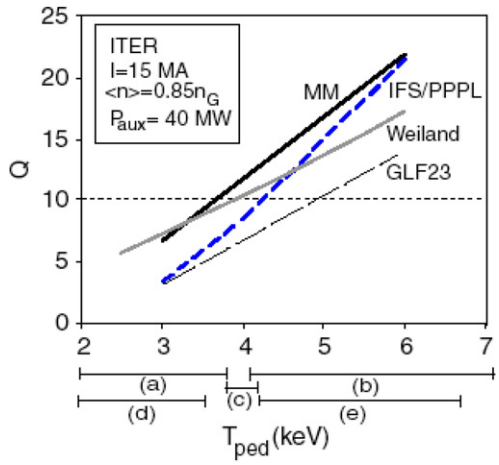

Figure 5. Q versus T_{ped} (ion temperature at the pedestal top) predicted for ITER by the MM, IFS/PPPL and GLF23 transport models at the same input parameters [13]. Also shown are predictions of the Weiland model at similar input parameters. Horizontal bars indicate the ranges of pedestal temperatures predicted by different pedestal scalings (chapter 2, section 4.2.1 [8]).

(neoclassical transport theory) by a large factor, typically one or two orders of magnitude. The exceptions are improved confinement modes, where the ion heat transport is often reduced to a neoclassical level. This transport enhancement was attributed to turbulent processes, but prior to the writing of the IPB, little comparison was made between experimental measurements and turbulence theory. More recently a wide range of experiment to theory/simulation comparisons have been conducted in core plasmas (chapter 2, section 2.3 [8]) using a variety of fluctuation diagnostics. Our confidence in the transport model driven by drift wave turbulence is improved by the correlation of core turbulence reduction and confinement improvement with relative changes in the growth and damping rates of the instabilities (ion temperature gradient (ITG) mode, trapped electron mode (TEM), electron temperature gradient (ETG) mode), the identification of zonal flow activity (e.g. geodesic acoustic mode (GAM)), the evidence for $E \times B$ velocity shear suppression of turbulence and turbulent transport and its effect upon the fluctuation parameters. Figure 4 shows a reasonable agreement of the frequency predicted for GAM oscillation and measurement [12].

Theory-based core modelling of ion temperature profile shows good agreement with measurement, suggesting that the ion temperature profile is stiff (i.e. the profile shape is quasi-invariant) as predicted by ITG mode theory. This suggests that temperatures at the top of the pedestal play a determining role on the plasma performance. Figure 5 shows the fusion gain projected from theory-based core transport models, as a function of ion temperature at the pedestal top [13]. This analysis shows that $Q > 10$ can be obtained in ITER inductive operation for pedestal temperatures >4 keV (see section 3.4). Attempts have been made to develop integrated models which incorporate the core, pedestal and SOL (scrape-off layer, the plasma connected to the divertor or limiter along the field line)/divertor regions, and these predict $Q \sim 10$ in the reference inductive operation (chapter 2, section 5.5.5 [8]). Results of dimensionless analysis, based on an appropriate JET DT discharge, also support the possibility of achieving $Q > 10$ in ITER (chapter 2, section 5.4 [8]).

Toroidal momentum transport in tokamaks is generally found to be anomalous and the viscosity is reduced in the internal transport barrier, as are other transport coefficients of heat and particles (chapter 2, section 3.5 [8]). Spontaneous rotation is observed without any momentum input, which can be qualitatively understood as a result of off-diagonal elements of the transport matrix. The understanding of toroidal momentum transport is still at a rudimentary stage; quantitative prediction to ITER requires further study.

3.2. Core confinement, transport and steady-state operation with weak or negative magnetic shear

At the time of writing the IPB, improved confinement regimes with a weak or negative magnetic shear were being developed. The enhanced performance of these plasmas was transient at that time. In the last few years, significant progress has been achieved in developing the weak magnetic shear regimes with high β_{N}, large fraction of the bootstrap current and improved energy confinement over the H-mode scaling sustained for a quasi-steady-state period. These regimes are promising for hybrid and steady-state operation in ITER.

The ordinary hybrid operating mode planned for ITER is based on a combination of inductive and non-inductive current drive, leading to a long pulse operation (>1000 s) with a significant fusion power (>300 MW, $Q = 5$) at a medium safety factor ($q_{95} = 3.3$) and conservative confinement assumption ($\mathrm{H}_{\mathrm{H98}(y,2)} = 1$) [4].

Recently, high beta and high confinement have been obtained in many tokamaks with weak magnetic shear with $\mathrm{H}_{\mathrm{H98}(y,2)} = 1.2$–$1.6$, $q_0 = 1$–1.5 and $q_{95} = 3.5$–4.5, in the absence of sawteeth (chapter 6 of this issue [9]). Figure 6 shows that high β_{N} of 2.5 is maintained for 16.5 s [14]. A higher beta limit is a key feature of these scenarios. The combination of a lower current and a lower loop voltage would allow operation with a high fusion gain for very long

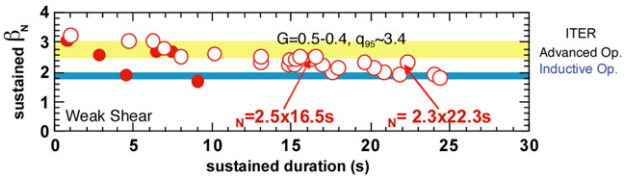

Figure 6. Sustainment of high β_N in JT-60U; the sustained β_N is plotted against the sustaining duration. The closed circles indicate the results obtained before the 2002 IAEA Conference, while the open circles represent the results after the 2002 IAEA FEC [14]. The improvement in heating and control has resulted in the longer sustainment of high beta state. The gradual reduction in beta is due to deterioration of confinement as a result of wall saturation.

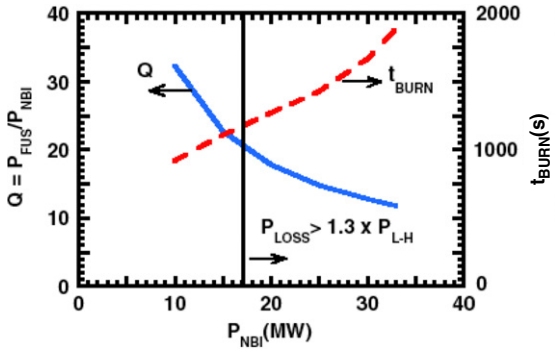

Figure 7. Fusion gain and burn time versus NBI power with a plasma current of 12 MA at HH = 1.2 and density of 85% of Greenwald density [16].

pulse duration. Strong impurity accumulation has not been observed in this mode. The quasi-stationary improved hybrid regimes with ~50% non-inductive current fraction at $\beta_N \sim 3$ that is close to the no-wall beta limit have been obtained. $H_{H98(y,2)} = 1.2$ is observed at $n/n_G = 0.85$ [15]. If ITER could achieve similar normalized parameters, fusion powers of ~350 MW, $Q > 10$ would be expected at $\beta_N \leqslant 2.2$ (figure 7) [16]. The required β_N is well below the no-wall ideal MHD limit. A burn time longer than 1000 s with $Q \sim 20$ could be reached (figure 7). This operation scenario is a potential candidate for an operation mode with high Q, long pulse, benign ELMs and no strong impurity accumulation.

For the steady-state (SS) operation, the total plasma current at the current flat-top phase should be generated non-inductively by the bootstrap effect, neutral beam injection (NBI) and RF waves. SS scenarios rely upon discharges with a relatively low plasma current, high safety factor $q_{95} \geqslant 4$, improved confinement ($H_{H98(y,2)} \geqslant 1.3$) and high beta ($\beta_N \geqslant 2.5$) (chapter 6 of this issue [9]). The improved confinement is expected to be achieved, e.g. in reversed-shear operation. Stationary operation has been obtained experimentally at $q_{95} \geqslant 5$, with the maximum performance just in line with ITER requirements for steady-state operation at $Q \sim 5$. Operation in these regimes requires strong plasma shaping and simultaneous control of the current and pressure profiles (chapter 6 of this issue [9]) and active control of RWMs and possibly NTMs (chapter 3 of this issue [17]).

A dimensionless parameter $G = \beta_N H_{89}/q_{95}^2$ is considered to be the figure of merit for evaluating inductive, hybrid and steady-state scenarios (chapter 6, section 6.2.1 [9]). H_{89} is the confinement enhancement factor relative to an L-mode

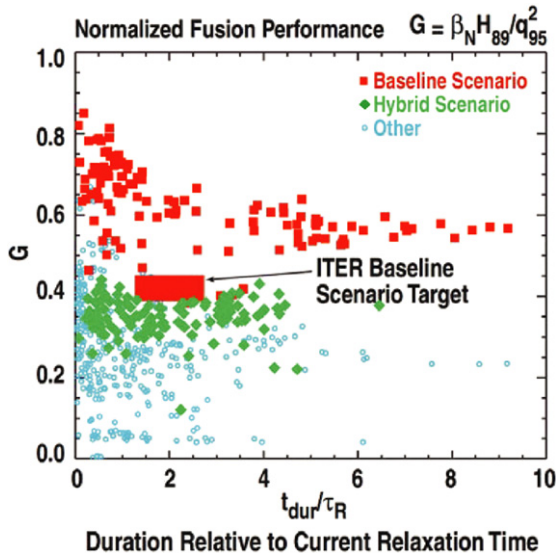

Figure 8. Plasma performance figure of merit versus duration normalized to current diffusion time (DIII-D). The filled squares are ITER baseline scenario discharges, the filled diamonds are hybrid scenario discharges and the open circles are other types of discharge [18].

scaling. This figure of merit ranges typically from ~0.25 (steady state) to 0.4 (conventional H-mode) and shall be ⩾0.4 for the 'hybrid' scenarios. The development of hybrid scenarios on several tokamaks, allowing steady operation at higher beta limits than those for the reference ELMy H-mode, has been quite remarkable in the recent years. Steady values of $G \geqslant 0.4$, corresponding to $Q \sim 10$ in ITER, have been achieved on several experiments for many current relaxation times (figure 8) [18].

Thanks to a better understanding and modelling of heating and current drive actuators and to real-time data processing on key parameters such as the current profile, sophisticated algorithms have been developed for the active control of steady-state and hybrid scenarios (chapter 8 of this issue [19]). One of the main remaining issues is the development of scenarios, or of algorithms, resulting in the lowest possible demand on control in terms of additional power.

Many areas require further work, in particular, the extrapolation of improved hybrid regimes to lower ρ^*; the size scaling of ITB formation and sustainment of ITBs at high plasma density, $T_i \sim T_e$ and slow toroidal rotation with prevention of impurity accumulation. An important effort remains to be done to achieve fully integrated scenarios, i.e. scenarios that are also compatible with the partially detached divertor condition of a burning physics device (the divertor plasma has to be partially detached to reduce heat loads on the divertor targets to acceptable levels (IPB chapter 4 [20])). In particular, steady-state scenarios privilege operation at relatively low density and high electron temperature to optimize the current drive efficiencies. Generally, steady-state and hybrid scenarios that can be considered for ITER have made impressive progress since the IPB; the domain is in full progress and new scenarios allowing the remaining issues to be progressively alleviated are being proposed.

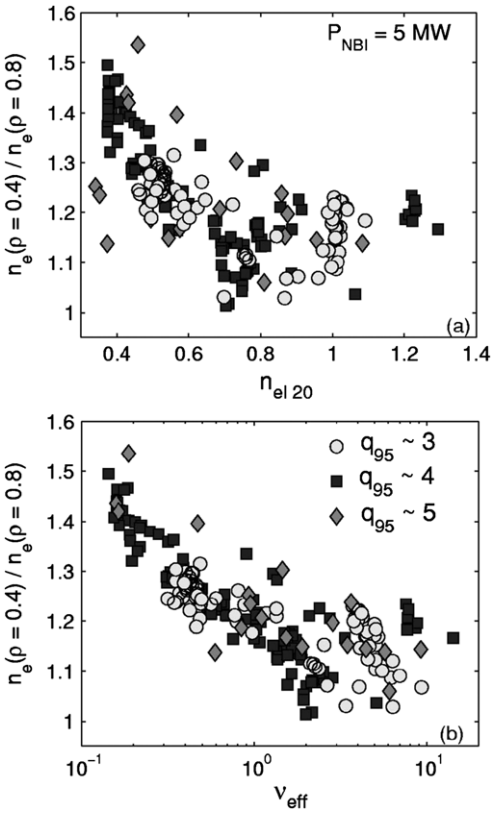

Figure 9. Density peaking, defined as $n_e(\rho = 0.4)/n_e(\rho = 0.8)$ versus the line average density ~in 10^{20} m^{-3}, panel (*a*), and versus $\nu_{\rm eff}$, panel (*b*), for the subset of stationary plasmas in the AUG H-mode database, with total NBI heating power of 5 MW. Different values of q_{95} are plotted with different symbols [21].

3.3. Particle and impurity transport (chapter 2, section 3.4)

Progress in particle transport studies has been slower than in heat transport studies because of the complication of the mixture of two sources (NBI in centre and gas-puffing and recycling at the edge) and involvement of convective transport. However, particle transport is very important in burning plasmas, since the density profile affects fusion performance and consequently plasma profile and stability. Global particle transport studies separating core and edge transport have shown that the core particle confinement improves with density while edge particle confinement deteriorates with density. Local particle transport studies show that the particle flux is described with a summation of diffusive and inward convective terms. In many cases these transport coefficients are anomalous. Some experiments show strong variation of the $D/\chi_{\rm eff}$ ratio, between 0.3 (at high density and low q_{95}) and 2.0 (at low density and high q_{95}), whereas other experiments show that this ratio is constant (the ratio varies from 0.15 to 0.25 in one experiment and ~1 in the other). A particle pinch at low collisionality has been observed in a number of devices and explained in the framework of the ITG/TEM transport theory or neoclassical theory (Ware pinch), but a clear experimental evidence for the existence of an anomalous inward pinch was shown, where peaked density profiles without central fuelling were observed with zero loop voltage. The density profile is shown to peak with lower collisionalities (figure 9) or edge heating but flattens with higher collisionalities or

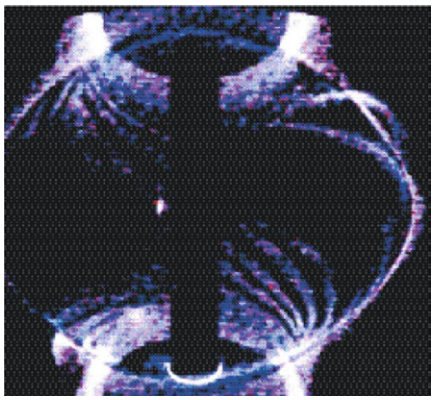

Figure 10. Filamentary structure of ELMs displayed in MAST [23].

central heating [21]. A theory-based model that explains these observations is still under development [22].

Impurity transport is a critical issue in burning plasma regimes due to possible fuel dilution and radiative cooling in the core. In ELMy H-mode plasmas, the impurity transport is reduced compared with L-mode, but impurity accumulation at the centre is usually not observed. With a relatively flat electron density profile, hollow profiles of impurities are observed, which is consistent with neoclassical temperature gradient screening, which should have a favourable effect on higher Z impurity profiles in low collosionality plasmas such as ITER even when turbulent diffusivity dominates over neoclassical. However, impurity accumulation at the centre is observed in enhanced confinement regimes with ITBs. These plasmas are characterized by a steep density gradient at the ITB. The central accumulation of high Z impurities tend to be more pronounced than low Z impurities. These observations are consistent with neoclassical theory. The application of ECH or ICH inside the ITB region has been shown to be effective in reducing the level of density peaking and consequently impurity accumulation.

3.4. Edge pedestal and ELMs (chapter 2, section 4)

At the time of IPB, H-mode pedestal investigation has already revealed that the maximum pressure gradient is usually consistent with ideal ballooning mode stability at the edge. The parameter dependence of pedestal width was not clear. Recent investigation shows that the edge pedestal gradient is consistent with peeling–ballooning mode theory. Figure 10 illustrates the filamentary structure of ELMs [23] (chapter 2, section 4.8.3 [8]); this observation is in agreement with the model theorizing that the ELMs are driven by medium-to-high n peeling–ballooning mode. We do not yet have a quantitative theory on pedestal width validated against experiments. Several empirical formulae have been proposed for the pedestal pressure to be used in the projection to ITER. Figure 11 shows an empirical scaling of pedestal pressure compared with experiments and extrapolated to ITER [24] (chapter 2, section 4.2.3 [8]). This projection suggests that a pedestal temperature of 5.3 keV can be achieved in ITER, satisfying a requirement of the pedestal temperature (higher than 4 keV) for $Q \sim 10$ in inductive operation (chapter 2, section 5 [8]).

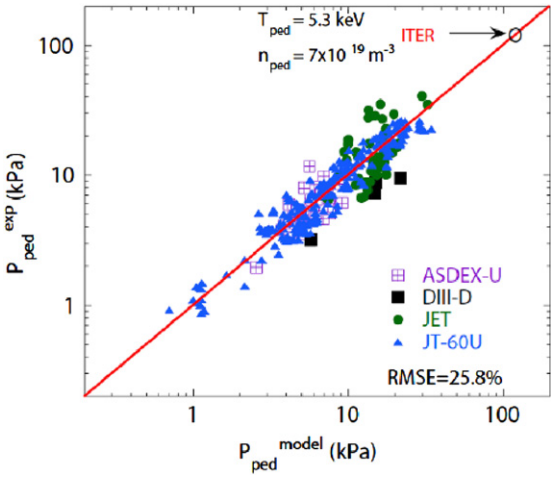

Figure 11. Comparison of pedestal pressure values in PDB3V2 database (chapter 2, section 4.3.2. [8]) with the model given in section 4.2.3 [24]. This model predicts $T_{\rm ped} = 5.3$ keV for ITER at $n_{\rm ped} = 7.0 \times 10^{19}$ m^{-3}.

3.5. Stabilization of neoclassical tearing modes (NTMs) (chapter 3, section 3.2.2)

NTMs, internal MHD instabilities driven by a deficit of bootstrap current at rational $q = m/n$ surfaces, are frequently observed in present-day positive shear plasmas, i.e. during ELMy H-mode operation (the basis for the ITER inductive scenario). Unconstrained growth of NTM modes can lead to deterioration of energy confinement and sometimes eventual disruption. The threat of NTMs to ITER operation in both the inductively driven ELMy H-mode scenario and in the similar hybrid scenario has been recognized since the time of the writing of the IPB. In the IPB, the possibility (and necessity) of controlling NTM growth through the use of local electron cyclotron current drive (ECCD) was highlighted as an inductive-scenario enabling element. Experiments conducted in a number of tokamaks have conclusively demonstrated the feasibility of using well-controlled ECCD to suppress NTM growth and/or prevent onset of the instability. Figure 12 shows the first demonstration of $m/n = 3/2$ NTM suppression using ECCD [25]. Active control techniques to track the position of the rational q surface and target the ECCD at the desired location have been demonstrated. Assessments of the ECCD requirements and ECCD deposition control needed for the control of NTMs ($m/n = 3/2$ and 2/1) in ITER inductive and hybrid scenarios have been developed. Present estimates suggest that NTM can be suppressed with an ECCD power of 10–30 MW in ITER. The overall prognosis based on successful suppression of NTMs in ITER is found to be well in hand.

3.6. Feasibility of sustained operation above the no-wall ideal MHD beta limit (chapter 3, section 3.2.3)

The ITER steady-state scenarios require plasma operation with beta values close to or above the so-called no-wall ideal MHD beta limit (the no-wall limit). For the plasma current profiles anticipated for ITER steady-state operation, the no-wall limit is calculated to be about $\beta_{\rm N} = \sim 2.4$, while the required $\beta_{\rm N}$ is $\geqslant 2.6$. In the presence of a nearby resistive wall, the manifestation of exceeding the no-wall limit is the development of a resistive wall mode (RWM), whose growth time is set by the wall resistive time (typically a few ms in present tokamaks and ~0.3 s in ITER). However, with sufficient plasma rotation velocity, growth of the RWM is suppressed and plasma operation well above the no-wall beta limit can be obtained. This behaviour has been well known since before the time of the writing of the IPB. The ability of these plasmas to exceed the ideal MHD no-wall beta limit for many wall times is now, in retrospect, well understood in terms of the effect of rotational stabilization of the RWM growth.

The failure of rotational stabilization and onset of a beta-limit disruption with application of increasing levels of non-axisymmetric error field was also reported, but not understood, in the IPB. Since then, this apparent dependence of the resistive wall beta limit on error-field level has been conclusively elucidated in terms of resonant field amplification (RFA), a collateral effect of RWM onset, wherein plasma operation near or slightly above the no-wall ideal limit results in an RWM-mediated amplification of natural or externally applied error fields. If the level of the amplified field becomes high enough, the resulting rotational drag slows the plasma rotation below the critical frequency needed to suppress RWM growth and a plasma energy confinement collapse and/or disruption ensues. The close agreement of predicted and observed RFA values in itself constitutes a rather elegant and conclusive confirmation of the underlying basic RWM theory. Correction (nulling out) of external error fields avoids the rotation braking caused by RFA and allows sustained plasma operation—with sufficient plasma rotation drive—at $\beta_{\rm N}$ values well above the corresponding no-wall limit.

The error-field correction capability in ITER should enable stabilization of the RWM by rotation especially when the rotation is large. However, given the relatively low external momentum input in ITER, feedback stabilization of the RWM by saddle coils is implemented.

The DIII-D tokamak is equipped with a set of 12 internal single turn feedback coils to provide fast feedback control of the RWM in those plasmas in which the rotation is below the threshold. Figure 13 shows that direct feedback has sustained a plasma with $\beta_{\rm N}$ almost 4 well over the no-wall limit for over 1 s [26].

The suppression of RWMs has been investigated for ITER steady-state scenarios. A multi-input, multi-output linear quadratic Gaussian (LQG) controller has been produced on the basis of a semi-analytical model of RWM with a code treating the configuration of the plasma, saddle coils and vacuum vessel. Analyses show that this controller, without using the second time derivative of the measured perturbed field, is able to suppress highly unstable modes with $C_\beta \sim 0.6$–0.8 ($C_\beta = (\beta_{\rm N} - \beta_{\rm N}(\text{no wall}))/(\beta_{\rm N}(\text{ideal wall}) - \beta_{\rm N}(\text{no wall}))$) with coil voltages of about 300 V/turn, which is implemented in ITER.

3.7. Feasibility of disruption mitigation using massive gas injection (chapter 3, section 3.3.6)

All tokamaks including ITER are inherently susceptible to disruption, which can bring large heat and electromagnetic loads and nearly complete conversion of thermal plasma current to relativistic (~10 MeV) suprathermal runaway

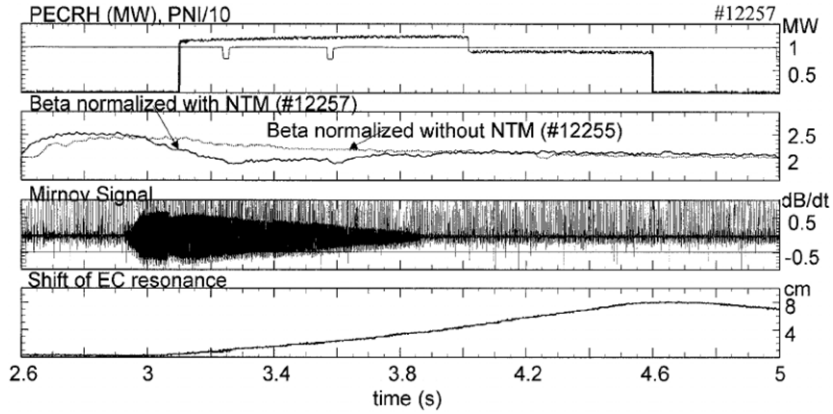

Figure 12. Decreasing amplitude of $m/n = 3/2$ Mirnov coil signal shows that the NTM is suppressed during ECCD [25]. The high frequency oscillations of the Mirnov coil signal are due to ELMs. The shift of the EC resonance position due to the variation of the toroidal magnetic field is given, and β_N of this discharge is compared with a (nearly) identical discharge without ELMs.

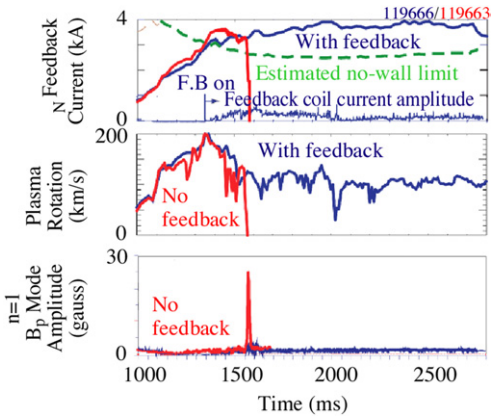

Figure 13. Direct feedback in DIII-D enables sustained operation well above the no-wall limit when plasma rotational stabilization is insufficient [26].

electron current. In ITER, disruptions have no 'single-event' potential to damage the plasma-facing components to failure. However, repetitive worst-case disruptions are not acceptable, since disruptions would shorten the life time of plasma-facing components and the deterioration of wall condition after disruption would reduce the availability of the machine. In Demo, very low probability of disruption (less than one disruption per year) and/or reliable active measures of disruption avoidance is assumed due to its serious consequences [27]. Thus disruption control constitutes an essential element for high availability of operation and long lifetime of plasma-facing components in ITER and elimination of disruptions in ITER would be essential for the high reliability of Demo.

In the IPB, the injection of massive neutral gas, equivalent to increasing the plasma electron density by a factor of about 200 (to a final density of about 2×10^{22} electrons m^{-3}) was identified as a possible disruption mitigation means. But at that time there was no experimental or theoretical precedent to believe that this high degree of density increase could necessarily be achieved, or achieved without in itself causing a disruption. However, recent gas-injection experiments in several medium-sized tokamaks, using massive quantities of either neon or argon gas have demonstrated that it is feasible to reach (or closely approach) the required electron densities and that the resulting rapid radiative cooling of the plasma also limits conduction of the plasma thermal energy to the divertor targets and reduces the magnitude and toroidal asymmetry of the halo currents that disruptions normally cause. The technique of massive gas injection appears to offer good promise for simultaneous mitigation of disruptions and runaway conversion in all ITER plasma operation scenarios.

For the case of a vertical displacement event, which occurs when the vertical position control is lost, the vertical movement is slow (the time scale ~0.5 s) in ITER, which ensures a high reliability of detection and mitigation. For the case of disruption, neural networks are being developed which trigger the mitigation system. In the long term, a disruption avoidance system should be developed.

3.8. Digital plasma control systems (chapter 8)

Since the writing of the IPB, the development of very sophisticated and comprehensive digital plasma control systems has taken place in most major tokamak facilities. These systems, which typically comprise a number of generic PC-type computers running asynchronously with real-time operating systems and interconnected with a fast GB/s network, have allowed a variety of plasma control and real-time diagnostic data utilization tasks to be undertaken in a fully digital manner. The types of control performed in this manner range from routine plasma current, position and equilibrium control, plasma density control and beta control to sophisticated multi-actuator control of the plasma safety factor profile and internal transport barrier location. Capabilities now possible include use of essentially real-time equilibrium reconstruction data for plasma shape and position control and divertor strike point control, incorporation of real-time MSE data in plasma current profile control algorithms and implementation of sophisticated algorithms to detect and track the location of NTMs for ECCD control of MHD stability.

The ability of the present generation of plasma control system to control the plasma parameters is now at a state that is basically limited only by the availability of diagnostic measurements and the corresponding 'actuators' needed to modify the parameters, even in a multiple-input, multiple-output algorithm sense. The required control system capability

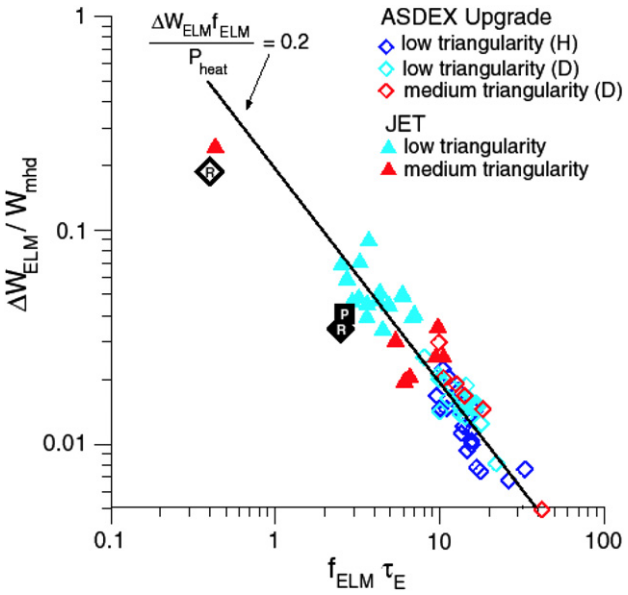

Figure 14. Comparison of ELM sizes obtained in this study for 19 Hz pellet triggered (P in filled black square) and 3 Hz (R in open black diamond) and 20 Hz (R in filled black diamond) intrinsic ELMs to values from a type-I ELM scaling for ASDEX Upgrade and JET [28].

(and many representative algorithms) is already available for ITER plasmas.

3.9. Particle control and power dispersal (chapter 4)

The heating power that the fusion plasma produces and supplied externally needs to be eventually exhausted at the edge. Since the wetted surface area is expected to be $\sim$4 m^2 at the target in ITER, 80 MW heat loss through the separatrix of ITER would result in an average power density of 20 MW m^{-2} at the target. In order to keep the peak target power density below $\sim$10 MW m^{-2}, a substantial reduction of the heat load is required. Also particle exhaust by divertor is required to control the density and purity of the core plasma. At the time of IPB writing, divertor code calculations suggested the feasibility of radiative cooling enhanced by partial detachment with ITER parameters. This provided optimism that inter-ELM heat load handling and particle exhaust would not be a problem for ITER. ELMs were expected to cause a serious heat load on the divertor but a quantitative analysis was yet to be made and an ELM mitigation scheme was yet to be developed.

Quantitative estimates based on experimental database have shown that power fluxes on the ITER divertor targets associated with type-I ELMs could be close to or above marginal for an acceptable divertor lifetime, which has motivated development of back-up scenarios. Potential scenarios include those with more frequent, smaller ELMs triggered by frequent pellet injection, edge ergodizaiton and regimes with benign or no ELMs (type II or grassy ELMs).

The idea of ELM-pacemaking (chapter 4, section 2.7.3 [29]) stems from the experimental observation that the amplitude of intrinsic ELM decreases with ELM frequency (figure 14) [28]. The ELMs induced by small pellets show similar amplitudes as the intrinsic ELMs. Analysis with ITER parameters suggests that reduction of ELM amplitude to a level acceptable for divertor targets is possible with such ELM-pacemaking at a frequency of 4 Hz or above. The ITER design includes pellet injectors on the high field side for fuelling and on the low field side for ELM-pacemaking. However, confinement deterioration is observed at frequent pellet injection and is a concern for ITER.

Magnetic perturbation induced by saddle coils can make edge magnetic islands overlap with each other, which enhances the transport in the pedestal, keeping the pressure gradient below the critical level to induce ELMs at safety factors $\sim$3.7 [30], (chapter 2, section 4.9.2 [8]). The saddle coils located inside the vacuum vessel are under study, but such in-vessel coils are associated with engineering difficulties in ITER. ELM suppression with out-vessel coils should be investigated. ELM suppression at a safety factor $\sim$3 is yet to be demonstrated. Possible triggering of NTM and consequences of elimination of toroidal rotation also need to be investigated.

Furthermore, improved confinement regimes free of type-I ELMs have been explored. For example, figure 15 shows that highly shaped, moderate q ($q_{95} \sim 4$) and high β_p ($\sim$1.6) discharges are associated with benign ELMs (chapter 2, section 4.7.5 [8]) [31]. The enhanced D-alpha (EDA) regime (chapter 2, section 4.7.2 [8]) has been observed along with its quasi-coherent modes. However, the viability of this regime is unlikely in ITER because of the low edge temperature that is required. The quiescent H (QH) mode (chapter 2, section 4.7.3 [8]) shows ELM-free discharges with good confinement. However, extrapolation to ITER is uncertain without a reliable physics-based model. High impurity levels of QH-plasmas are also a concern.

The plasma-facing components for the initial operation consist of the following; the divertor targets are covered by carbon-fiber-composite (CFC) graphite; tungsten is used at the dome and baffle (upper target) regions for its low yield of physical sputtering by neutral particles; beryllium is used for the first wall for its small impact on the plasma performance and high oxygen gettering. CFC targets are commonly used as plasma-facing components in present-day experiments due to its compatibility with a wide range of plasma parameters. However, tritium retention control, required with CFC targets, remains a key issue and more efforts are called for to investigate retention mechanism and develop efficient removal techniques. Early experiments with a horizontal target and with a limiter configuration suggested that $\sim$30% of tritium injected is retained in the vessel with C walls and divertor targets. If we simply extrapolate this data to ITER, the T retention reaches a project guideline (limit on the amount of T) rather quickly. However, recent experiments with vertical target show that $\sim$3% of injected tritium is retained in the vacuum vessel: one order of magnitude reduction of the build-up rate. Furthermore, it was shown that the build-up of tritium retention could be significantly reduced by a factor of $\sim$1/5 by the coverage of carbon surface by beryllium. The level of tritium retention predicted for ITER is thus reduced but the uncertainties are large and the methods for its removal need more development. The primary challenge is to remove tritium from shadow areas, not accessible by plasma, as well as from surfaces with mixed material deposition (e.g. Be/C/W).

Elimination of graphite from the vessel would be attractive from the viewpoint of tritium retention control. High

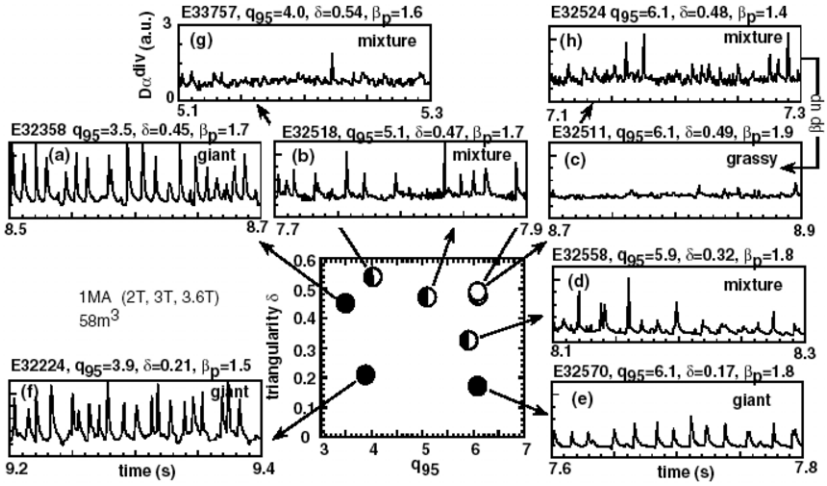

Figure 15. Change of ELM activity (divertor D_α signal) with δ, q_{95} and β_p at $I_p = 1$ MA ($\Delta t = 0.2$ s in all cases). Giant ELMs are replaced by grassy ELMs as q_{95} increases with fixed δ and β_p ((*a*) to (*b*) to (*c*)); as δ increases with fixed q_{95} and β_p ((*e*) to (*d*) to (*c*)); and as β_p increases with fixed δ and q_{95} ((*h*) to (*c*)). Compared with (*b*) ($\delta = 0.47$ and $q_{95} = 5.1$), an almost grassy ELMy phase appears at a higher $\delta = 0.54$ even at a low $q_{95} = 4$ (*g*) [31].

Z materials such as tungsten are attractive for their long lifetime and are deemed most applicable to a fusion reactor. However, experiments with tungsten [32] show that tungsten can accumulate in the centre in discharges with an ITB and/or with a peaked density profile (figure 16) in the absence of sawtooth/fishbones and frequent ELMs (chapter 4, section 2.5.4.1 [29]). It has also been demonstrated that high central heating could suppress the accumulation (figure 16). Further experimental studies with all high Z plasma-facing components in large and medium-sized tokamaks are required to investigate the specific restrictions that tungsten may impose on ITER operation. Surface melting after disruption and subsequent formation of irregular surfaces are of serious concern, since heat loads during disruption in ITER are estimated to be one or two orders of magnitude higher than in the present machines and these irregular surfaces can easily melt or evaporate at normal operation. Therefore further efforts should be made in the development of disruption prediction, mitigation and avoidance. Since adoption of tungsten might limit plasma operational flexibility, the tungsten target is not suitable for the initial operation, in which a wide operational space is fundamental. After establishing reliable operation modes, it would be better to replace CFC targets with tungsten to facilitate tritium retention control and to demonstrate a target suitable for a next-generation reactor and it may be better to replace the beryllium first wall with tungsten at least partially. Development and validation of theory-based models of impurity transport is also useful for the assessment of plasma performance with tungsten. The current combination of CFC/tungsten targets and beryllium walls is expected to minimize T retention and W erosion with a wide range of parameters, which is essential for the initial operation.

Dust of sizes ranging from 10 to 0.1 mm is observed in tokamaks. Dust has recently attracted attention in light of its potential impact on safety in ITER, due to its high chemical reactivity and possible activation (chapter 4, section 2.6.5 [29]). Understanding of its formation mechanisms and measurement and removal methods need to be developed.

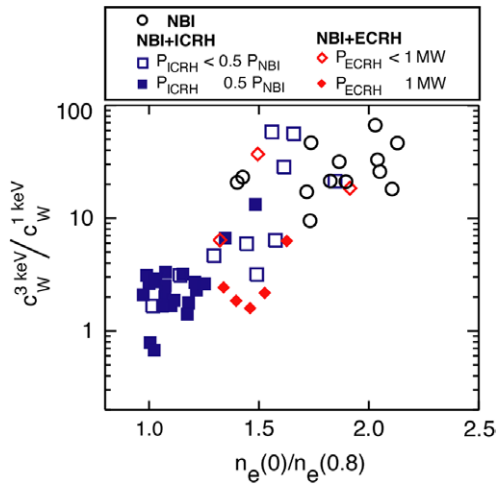

Figure 16. Peaking of the W concentration (c_W) as a function of peaking of background density [32]. Shown are the ratios of c_w at the location where the electron temperature is 3 keV to c_w at the location where the electron temperature is 1 keV. Discharges with pure NBI heating (black circles) show the strongest peaking, whereas central ECRH reduces the c_W peaking significantly already at low additional heating power.

3.10. Energetic particle physics (chapter 5)

One of the major scientific goals for ITER is to demonstrate and investigate burning plasmas, in which a significant power is produced by the DT fusion reactions. Such plasmas are characterized by a large isotropic population of fusion alphas, providing the dominant heating of the plasma. In DT plasmas, self-heating is provided by the α-particles generated at 3.5 MeV by the D-T fusion reactions. Other fast or energetic ions with energies in the MeV range, well above the thermal distribution of the plasma bulk, are generated by ion cyclotron resonant heating (ICRH) and NBI. The behaviour of energetic ions is a key subject of burning plasma studies. Transport and confinement of fusion α-particles not only impact machine performance by affecting the fusion yield but can also damage the first wall.

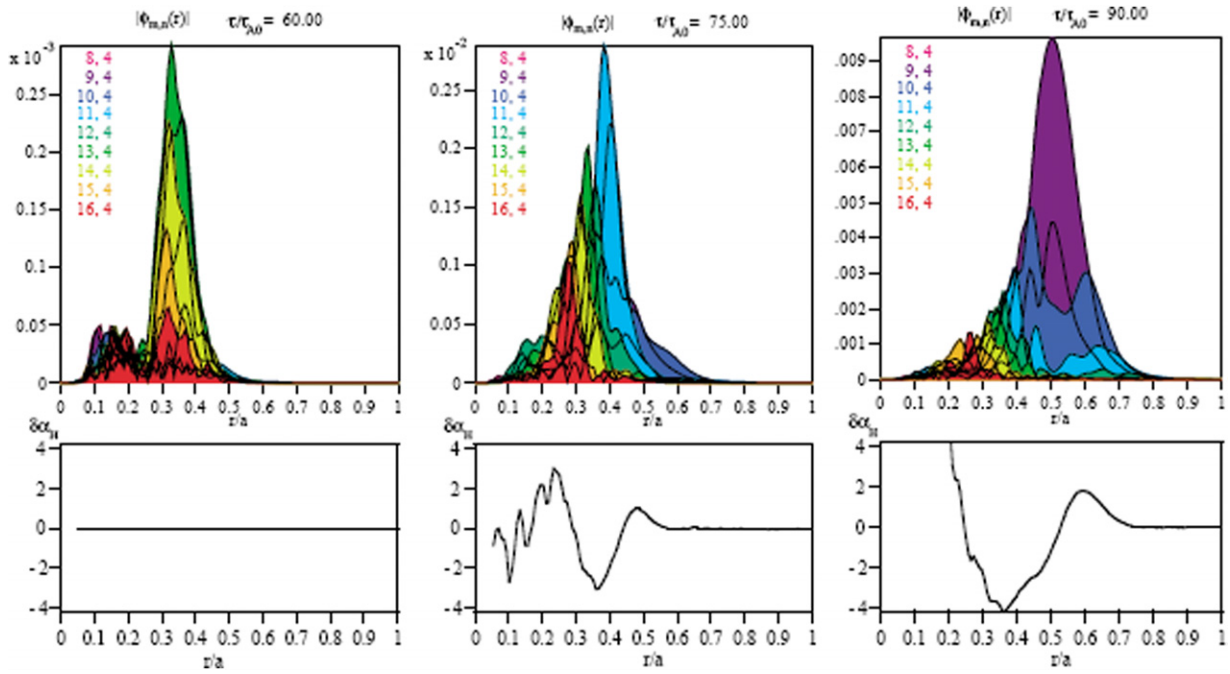

Figure 17. Time evolution of the EPM radial structure, decomposed in poloidal Fourier harmonics. Here $\tau_{A_0} = R_0/v_A$ ($r = 0$) (R_0 is the major radius and v_A is Alfven speed). The toroidal mode number is $n = 4$. The nonlinear modification of $\alpha_E^o - R_0 q^2 \rightarrow (d\beta_E/dr)$ (change in alpha particle pressure) is also shown [33].

A large effort was dedicated to the development of methods to simulate fusion born alphas in plasmas without significant fusion reactivity. Ripple losses are relatively well understood. The synergy between new observations and advanced modelling has led to an optimization of ferritic inserts in ITER to reduce ripple-induced α-particle losses with reversed-shear configurations to a negligible level.

The interaction of fast ions generated by additional heating with low frequency MHD has been investigated in a variety of experiments. The linear theory of kinetic ballooning modes and localized interchange modes is well advanced, and the behaviour with sawteeth is well described.

The field of linear stability thresholds for collective instabilities was advanced through a large number of experimental results and significant progress in theoretical simulations. Damping and drive mechanisms are qualitatively understood, although quantitative predictions for specific modes are still to be ameliorated, especially in regimes in which fluid and kinetic models give significantly different results.

The understanding of the nonlinear phase of the interaction between waves and fast ions was significantly improved, particularly in the weakly nonlinear regime. Figure 17 shows nonlinear interaction between energetic particle modes and alphas, suggesting potentially significant effect on alphas [33]. Measurements of the modes are used to extract information about the background plasma and/or the fast ion population. Although nonlinear modelling appears to be in qualitative agreement with experiments, limited information is available on the fast ion redistribution and losses, due to the difficulty in achieving large amplitude modes in present devices and in having sufficiently sensitive diagnostic tools to measure the energy and radial distribution of the fast ions.

3.11. Diagnostics (chapter 7)

ITER will require an extensive set of plasma and first wall measurements for machine protection, plasma control and physics evaluation. Because of the harsh radiation environment, diagnostic system selection and design involves a range of challenges not previously encountered: for example, radiation induced conductivity and radiation induced EMF in magnetic sensors mounted in the vacuum vessel, enhanced erosion of diagnostic first mirrors due to energetic particle bombardment and enhanced absorption and photoluminescence in windows and optical fibres. The diagnostic designs also have to satisfy stringent requirements on tritium confinement, vacuum integrity, remote handling maintainability and reliability. Access will be restricted and must maintain neutron streaming below allowable limits. Taken together, these aspects mean that the provision of diagnostics for ITER is arguably the most challenging undertaken thus far in the history of plasma diagnostics.

It is expected that there will be a phased introduction of powerful operation and advanced scenarios. The demands on the measurements will rise accordingly with more parameters being brought under real-time control. The parameters necessary to support the different planned operating scenarios—inductive ohmic L-mode, inductive ELMy H-mode, hybrid operation, and steady-state operation, as the operation advances through the H, D and DT phases—have been identified. For each parameter, detailed requirements (ranges, time and space resolutions, accuracies) have been developed and the full specifications are included in tabular form. In addition, for each parameter a justification has been prepared.

R&D is in progress to resolve the remaining issues. These include specific component testing, for example on prototype

Table 4. Initial set-up and possible upgrade scenarios of heating and current drive systems.

	Start-up Power (MW)	Scenario 1 Power (MW)	Scenario 2 Power (MW)	Scenario 3 Power (MW)	Scenario 4 Power (MW)
NB (1 MeV)	33	33	50	50	50
IC (40–50 MHz)	20	40	20	40	20
EC (170 GHz)	20[a]	40[b]	40[b]	40[b]	20[b]
LH (5 GHz)	0	20	20	0	40
Total	73	133	130	130	130

[a] 20 MW of EC will be used either in two upper ports to control neoclassical tearing modes, or in one equatorial port for main heating or current drive.
[b] EC will allow use of four allocated top ports for the power upgrade. No additional equatorial ports are therefore foreseen for this system. The total installed power is given in the table and the total maximum power into the torus is limited to 110 MW.

magnetic coils or bolometers, generic testing of candidate materials, for example in-vessel cabling, and testing of new diagnostic techniques which have the potential to be relatively rugged in the ITER environment. All optical/IR, spectroscopic and microwave systems view the plasma with a mirror and a critical issue is the lifetime of this component. Dedicated R&D is in progress on candidate first mirrors.

Finally, ITER will provide a unique opportunity of measurements in a fusion reactor environment. That experience will be useful for measurements of ITER plasma itself during operation with standard and enhanced performance and for diagnostics development for the next step device. It is probable that there will still be an extrapolation in plasma performance from ITER to the next step device. The experience gained on ITER will reduce the uncertainties in this extrapolation and provide the basis on which an informed choice of diagnostics can be made and diagnostic systems designed.

4. Summary

(1) The physics R&D after IPB are highlighted by significant progress in understanding of turbulent transport, theory-based modelling of core, H-mode confinement at $n \sim n_G$, improved helium exhaust modelling, sustainment of hybrid- and SS-relevant scenarios at high beta and confinement, ELM mitigation, NTM and RWM control, disruption mitigation, understanding of energetic particle modes and diagnostics development.

(2) These have contributed to improved feasibility of ITER achieving its goals. Especially, validation of core transport models has progressed and analysis with ITER parameters suggests that the achievement of $Q > 10$ in the inductive operation is feasible. Improved confinement and beta have been observed with low shear (= high β_p = 'hybrid') operation scenarios in many tokamaks. If similar normalized parameters were achieved in ITER, it would provide an attractive scenario with high Q (>10), long pulse (>1000 s) operation with beta < no-wall limit and benign ELMs.

(3) For improved physics understanding, more work remains in the areas of transport of momentum and particles and transport and stability in the edge pedestal and effects of TAE modes. Understanding of core impurity levels should also be developed. For reliable and high duty operation, further work is required to develop control schemes of disruption, ELM, impurity, NTM, RWM, dust and tritium retention.

(4) ITER provides a unique opportunity of investigating physical phenomena under reactor conditions, which are impossible to achieve in present machines. Continued physics R&D, focused on ITER-relevant topics, will reduce uncertainties of projection and help develop control schemes that will be essential for handling problems that may arise during ITER operation. Physics understanding, projection and control methodologies developed and validated in ITER and other machines will be important for paving the path for Demo.

Appendix A.

Appendix A.1. ITER

ITER is a long pulse tokamak with elongated plasma and single null poloidal divertor. The nominal inductive operation produces a DT fusion power of 500 MW for a burn length of 400 s, with the injection of 50 MW of auxiliary power. Its main features and characteristics of its heating systems are summarized in tables 2 and 4. The major components of the tokamak are the superconducting coils which provide toroidal and poloidal fields which magnetically confine, shape and control the plasma inside the toroidal vacuum vessel. The magnet system comprises TF coils, the CS, external PF coils and correction coils (CC). The vacuum vessel has a double-walled structure.

The tokamak fuelling system is designed to inject gas and solid pellets of hydrogenic isotopes (H_2, D_2, T_2 or DT). During plasma start-up, low-density gaseous fuel will be introduced into the vacuum vessel chamber by the gas-injection system. The plasma will progress from electron-cyclotron-heating assisted initiation, in a circular configuration touching the outboard limiter, to an elongated divertor configuration as the plasma current is ramped up. Once the current flat-top value (nominally 15 MA for inductive operation) is reached, subsequent plasma fuelling (gas or pellets) together with additional heating for ~100 s leads to a high Q DT burn with a fusion power of about 500 MW. With non-inductive current drive from the heating systems, the burn duration is envisaged to be extended to 1 h. In inductive scenarios, before the inductive flux available has been fully used, reducing the

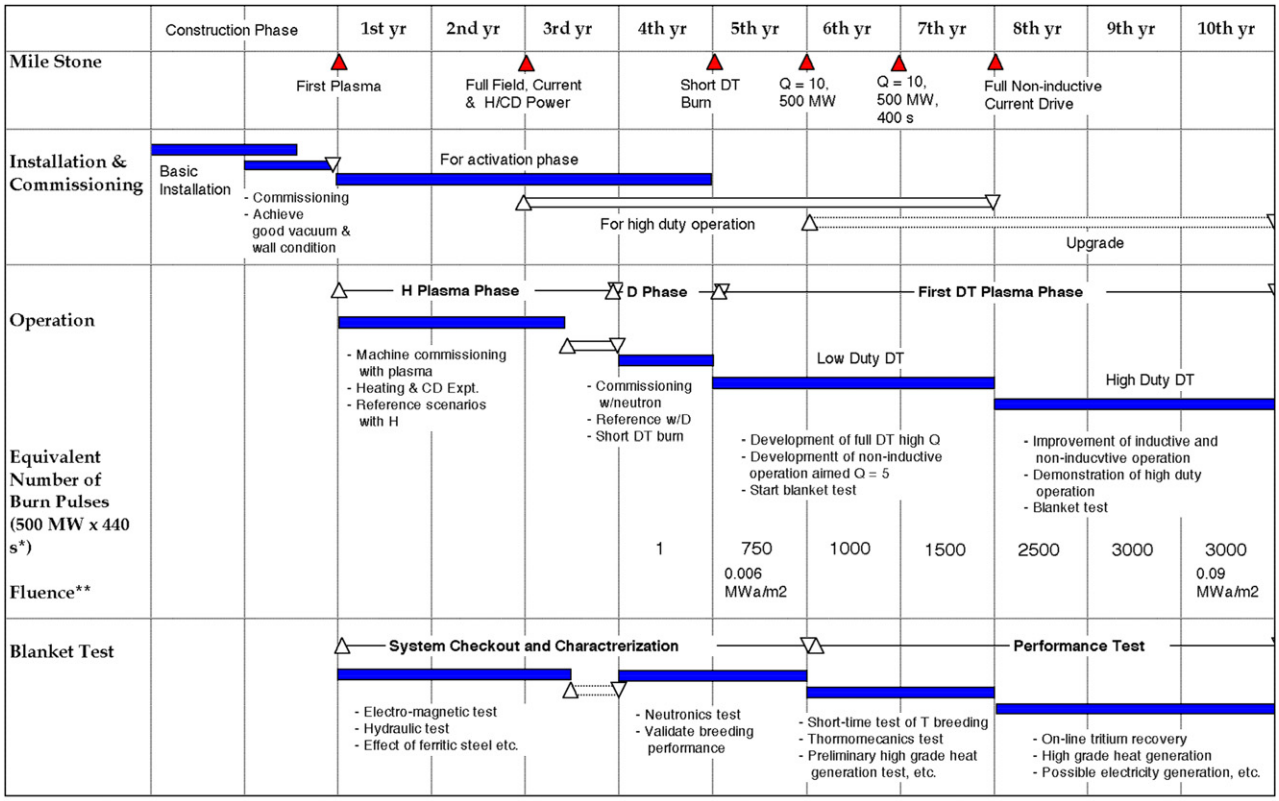

* The burn time of 440 s includes 400 s flat top plus 40 s of full power neutron flux to allow for contributions during ramp-up and ramp-down
** Average fluence at first wall (neutron wall load is 0.56 MW/m^2 on average and 0.77 MW/m^2 at outboard equator)

Figure 18. Initial operation plan of ITER.

fuelling rate so as to slowly ramp down the fusion power terminates the burn. This phase is followed by plasma current ramp-down and finally by plasma termination. The inductively driven pulse has a nominal burn duration of 400 s, with a pulse repetition period as short as 1800 s. The integrated plasma control is provided by the PF, pumping, fuelling (D, T and impurities such as N_2, Ar) and heating systems all based on feedback from diagnostic sensors.

Appendix A.2. Operation scenarios and phases

As an experimental device, ITER is required to be able to cope with various operation scenarios and configurations. Variants of the nominal scenario are therefore considered for extended duration plasma operation, and/or steady-state modes with a lower plasma current operation, with H_2, D_2, DT (and He) plasmas, potential operating regimes for different confinement modes, and different fuelling and particle control modes. Flexible plasma control should allow the accommodation of 'advanced' plasma operation based on active control of plasma profiles by non-inductive current drive, heating or fuelling.

An initial operation plan of the first 10 years is shown in figure 18. The first operation phase will be conducted with hydrogen or helium plasmas. During this phase, commissioning of various equipment will be completed, and a reference operation scenario will be developed. Adequacy of heating systems for L–H transition, divertor function will be confirmed and extrapolation of performance during the following DT phase can be made based on the confinement characteristics during the H_2-phase. Characteristics of transient phenomena, such as disruption, vertical displacement events and ELMs, will be investigated, and mitigation measures (impurity gas injection, pellet injection) will be tested. The neural network will be trained and tested for disruption prediction. Erosion and re-deposition of first wall and divertor materials will be investigated. Wall conditioning procedures will be developed including the procedures for tritium removal. Formation of dusts will be investigated and the dust removal techniques will be developed.

During the DT phase, a reference DT scenario will be developed by optimizing DT fuelling, fusion power, auxiliary heating power and burn pulse length. Exploration will be made in wide operation regimes to investigate burning plasmas and steady-state plasmas and reliable scenarios will be developed for long pulse engineering tests without severe disruptions, vertical displacement events and giant ELMs.

References

[1] ITER Physics Basis Editors *et al* 1999 *Nucl. Fusion* **39** 2137
[2] ITER Final Design Report, Cost Review and Safety Analysis 1998 *ITER Council Proc. (ITER Documentation Series* No 15*)* (Vienna: IAEA) p 39
[3] Technical Basis for the ITER Final Design Report, Cost Review and Safety Analysis 1998 *(ITER Documentation Series* No 16*)* (Vienna: IAEA)
[4] ITER Technical Basis 2002 *(ITER EDA Documentation Series* No 24*)*

[5] Mukhovatov V. *et al* 2007 Progress in the ITER Physics Basis *Nucl. Fusion* **47** S404–S413
[6] 1998 *ITER Council Proc. (ITER Documentation Series* No 15*)* (Vienna: IAEA) p 148
[7] Wesson J. *et al* 2003 *Tokamaks* (International Series of Monographs on Physics vol 118 (Oxford: Oxford University Press) (3rd version)
[8] Doyle E.J. *et al* 2007 Progress in the ITER Physics Basis *Nucl. Fusion* **47** S18–S127
[9] Gormezano C. *et al* 2007 Progress in the ITER Physics Basis *Nucl. Fusion* **47** S285–S336
[10] ITER Physics Basis Editors *et al* 1999 *Nucl. Fusion* **39** 2175 (Chapter 2, section 6.4)
[11] Sartori R. *et al* Scaling study of ELMy H-mode global and pedestal confinement at high triangularity in JET *Proc. 20th Int. Conf. on Fusion Energy 2004 (Vilamoura, Portugal, 2004)* (Vienna: IAEA) CD-ROM EX/6-3 and http://www-naweb.iaea.org/napc/physics/fec/fec2004/datasets/index.html
[12] McKee G.R. *et al* 2003 *Phys. Plasmas* **10** 1712
[13] Mukhovatov V. *et al* 2003 *Plasma Phys. Control. Fusion* **45** A235
[14] Suzuki T. *et al* 2004 *Proc. 20th Int. Conf. on Fusion Energy 2004 (Vilamoura, Portugal, 2004)* (Vienna: IAEA) CD-ROM EX/1-3 and http://www-naweb.iaea.org/napc/physics/fec/fec2004/datasets/index.html
[15] Sips A.C.C. *et al* 2003 *30th EPS Conf. on Controlled Fusion and Plasma Physics (St Petersburg, Russia, 2003)* vol 27A (ECA) O-1.3A
[16] Shimada M. *et al* 2004 *Proc. 20th Int. Conf. on Fusion Energy 2004 (Vilamoura, Portugal, 2004)* (Vienna: IAEA) CD-ROM IT/1-1 and http://www-naweb.iaea.org/napc/physics/fec/fec2004/datasets/index.html
[17] Hender T.C. *et al* 2007 Progress in the ITER Physics Basis *Nucl. Fusion* **42** S128–S202
[18] Wade M.R. *et al* 2005 *Nucl. Fusion* **45** 407
[19] Gribov Y. *et al* 2007 Progress in the ITER Physics Basis *Nucl. Fusion* **47** S385–S403
[20] ITER Physics Basis Editors *et al* 1999 *Nucl. Fusion* **39** 2391
[21] Angioni C. *et al* 2003 *Phys. Plasma* **10** 3225
[22] Angioni C. *et al* 2005 *Phys. Plasma* **12** 112310
[23] Kirk A. *et al* 2004 *Proc. 20th Int. Conf. on Fusion Energy 2004 (Vilamoura, Portugal, 2004)* (Vienna: IAEA) CD-ROM EX/2-3 and http://www-naweb.iaea.org/napc/physics/fec/fec2004/datasets/index.html
[24] Sugihara M. *et al* 2003 *Plasma Phys. Control. Fusion* **45** L55
[25] Gantenbein G. *et al* 2000 *Phys. Rev. Lett.* **85** 1242
[26] Okabayashi M. *et al* 2005 *Nucl. Fusion* **45** 1715
[27] Najmabadi F. *et al* 1997 *Fusion Eng. Des.* **38** 3
[28] Lang P.T. *et al* 2003 *Nucl. Fusion* **43** 1110
[29] Loarte A. *et al* 2007 Progress in the ITER Physics Basis *Nucl. Fusion* **47** S203–S263
[30] Evans T.E. *et al* 2004 *Phys. Rev. Lett.* **92** 235003
[31] Kamada Y. *et al* 2000 *Plasma Phys. Control. Fusion* **42** A247
[32] Neu R. *et al* 2005 *Nucl. Fusion* **45** 209
[33] Zonca F. *et al* 2002 *Proc. 19th Int. Conf. on Fusion Energy 2002 (Lyon, France, 2002)* (Vienna: IAEA) CD-ROM TH/4-4 and http://www.iaea.org/programmes/ripc/physics/fec2002/html/fec2002.htm